

Atomic-size effects on medium-range order in glasses

H. Iyetomi

Department of Physics, University of Tokyo, Bunkyo-ku, Tokyo 113, Japan

P. Vashishta

Concurrent Computing Laboratory for Materials Simulations, and Department of Physics and Astronomy, Louisiana State University, Baton Rouge, Louisiana 70803-4001

(Received 3 April 1992)

Effects of atomic sizes on structural correlations in AX_2 -type disordered systems such as SiO_2 , GeSe_2 , and Ag_2Se are studied using a charged-hard-sphere model and the hypernetted-chain scheme. Structural change is elucidated as a function of the size ratio through the first sharp diffraction peak in the number-number structure factor (medium-range correlations), the A - X coordination [formation of $A(X_{1/2})_4$ tetrahedra], and the principal peak in the charge-charge structure factor (charge ordering). We find a gradual change from SiO_2 -type to Ag_2Se -type disordered structure in the range of $0.5 < R < 1.0$, where $R (= \sigma_A / \sigma_X)$ is a ratio of the steric radius of A species to that of X species. As R increases, the medium-range order, which is closely related to the formation of $A(X_{1/2})_4$ tetrahedra, disappears. In the transition region frustration between the steric and Coulombic interactions depresses the charge ordering.

I. INTRODUCTION

In many oxide and chalcogenide glasses of AX_2 type, including SiO_2 , GeO_2 , GeSe_2 , and SiSe_2 , a first sharp peak is observed in the scattering functions.^{1,2} The position of the first sharp diffraction peak (FSDP) signifies medium-range correlations extending beyond nearest-neighbor distances. Moss and Price¹ gave a unified point of view for medium-range order on the basis of a random-packing model of basic structural units.

According to our previous study,^{3,4} medium-range order arises from a combination of steric and charge-transfer effects. Both effects are responsible for forming a structured network consisting of $A(X_{1/2})_4$ tetrahedra; the charge of an A atom sitting at the center of the tetrahedron is locally balanced by twofold-coordinated X atoms at the four corners. Such a conditional packing of atoms gives rise to medium-range order and the attendant FSDP. The FSDP essentially has a neutral character and is associated with correlations whose spatial extent is determined by local-charge neutrality. The appearance of the FSDP thereby does not depend on minor details in the atomic potentials. Essential features of the structural correlations in the glasses are thus preserved in a model comprising charged hard spheres.^{3,4}

The formation of such elementary units as $A(X_{1/2})_4$ tetrahedra reasonably depends on the fact that the steric radius of A -species atoms is much smaller than that of X -species atoms. As the difference in steric sizes decreases, it is expected that those building units are distorted and eventually destroyed, leading to the disappearance of medium-range order. In the opposite limit, namely, when A -species atoms are much larger than X -species atoms, there exists a different class of materials which are exemplified by Ag_2Se , Ag_2S , etc. These are

characterized as being superionic conductors at low temperatures.⁵⁻⁷ A question which naturally arises is, how is the network structure with medium-range order modified and transformed into a disordered structure, such as Ag_2Se has, as the relative sizes of atoms change?

In this paper, therefore, we adopt a AX_2 -type charged-hard-sphere model and study structural properties of the system with variation of the ratio of atomic radii. We pay a special attention to the following: the first sharp peak in the number-number structure factor associated with medium-range correlations, bond lengths and A - X coordination in connection with the formation of $A(X_{1/2})_4$ tetrahedra, and the main peak in the charge-charge structure factor reflecting charge ordering. For the calculation of the correlation functions, we use the hypernetted-chain (HNC) integral equation,^{8,9} the accuracy of which has been established in describing structural properties of long-ranged Coulombic systems.^{10,11}

Divalent-metal halides, including alkali-earth chlorides and ZnCl_2 , are another family of AX_2 -type materials which are essentially describable as mixtures of charged hard spheres. For specific materials, detailed structural analyses,¹²⁻¹⁴ combined with x-ray and/or neutron-diffraction data, have been done using sophisticated potential models.

We remark here that such a detailed comparison with experimental results is out of the scope of the present paper. Quantitative analysis of experimental data requires much more realistic potentials: Ingredients which have to be incorporated are softness of steric repulsion, charge-dipole interaction due to the large electronic polarizability of anions, three-body forces accounting for the covalent nature of bonding, and so forth.^{15,16}

Abramo *et al.*^{17,18} studied atomic-size effects on the correlation structure of a whole family of molten alkali

halides within the AX -type charged-hard-sphere model. Extensive comparison of the partial static-structure factors and x-ray-diffraction patterns was made with experimental results. Their calculations of the correlation functions are based on the mean spherical approximations (MSA's),¹⁹ which were developed for a fluid of charged hard spheres. The advantage of the MSA lies in that it yields direct analytic expressions for the correlation functions. The MSA, however, suffers from its limitations in predicting the radial distribution functions at short separations; the positivity of the radial distribution functions is not guaranteed in the MSA in contrast to the HNC approximation.

In the next section, the model used for this study is described. Section III contains a brief account of the HNC integral-equation scheme and numerical procedure for solving the equations. Results of the structural analyses are discussed in Sec. IV. A summary of this work is presented in Sec. V.

II. CHARGED-HARD-SPHERE MODEL

In the AX_2 -type system under study, we assume that atoms of ν species ($\nu = A$ or X) have a hard core of radius σ_ν and carry charge Z_ν . The overall charge neutrality imposes the relation, for the valences, $Z_A + 2Z_X = 0$. The interaction potentials $\phi_{\mu\nu}(r)$ between the μ th and ν th species atoms are then written as

$$\phi_{\mu\nu}(r) = \begin{cases} \infty & \text{for } r < \sigma_\mu + \sigma_\nu, \\ Z_\mu Z_\nu / r & \text{for } r > \sigma_\mu + \sigma_\nu. \end{cases} \quad (1)$$

By virtue of a scaling property, the equilibrium state of the system is completely characterized by a set of three parameters: the total packing fraction η , the Coulomb coupling parameter Γ , and the hard-core ratio R . These parameters for the system with temperature T are defined in the following way:

$$\eta = \frac{4\pi}{3} (c_A \sigma_A^3 + c_X \sigma_X^3) \rho, \quad (2)$$

$$\Gamma = \frac{|Z_A Z_X| / a}{k_B T}, \quad (3)$$

and

$$R = \sigma_A / \sigma_X. \quad (4)$$

Here c_ν is the concentration of ν -species atoms, ρ is the total number density, and the mean distance between particles, a , is defined by $(3/4\pi\rho)^{1/3}$.

For molten GeSe₂ near the melting point, the three parameters are taken to be $\eta = 0.44$, $\Gamma = 80$, and $R = 0.38$. These are optimized values so as to reproduce the experimental neutron-scattering function within the charged-hard-sphere model.^{3,4} Recently, Rino *et al.*²⁰ have worked out an effective potential for Ag₂Se which is applicable to the supersonic conductor phase as well as to the molten phase. Using the potential parameters, we can evaluate η , Γ , and R in the vicinity of the melting temperature of Ag₂Se as $\eta = 0.52$, $\Gamma = 31$, and $R = 3.1$.

III. HNC SCHEME

To calculate the correlation functions, we took advantage of HNC theory,^{8,9} as mentioned in the Introduction. The HNC equation for the partial pair-distribution functions $g_{\mu\nu}(r)$ of the system reads

$$g_{\mu\nu}(r) = \exp[-\phi_{\mu\nu}(r)/k_B T + h_{\mu\nu}(r) - c_{\mu\nu}(r)], \quad (5)$$

where $h_{\mu\nu}(r) [\equiv g_{\mu\nu}(r) - 1]$ refer to the total correlation functions. The direct correlation functions $c_{\mu\nu}(r)$ are related to $h_{\mu\nu}(r)$ through the Ornstein-Zernike relation²¹

$$h_{\mu\nu}(r) = c_{\mu\nu}(r) + \sum_\tau \rho_\tau \int d\mathbf{r}_1 c_{\mu\tau}(|\mathbf{r} - \mathbf{r}_1|) h_{\tau\nu}(r_1), \quad (6)$$

where ρ_τ is the number density of τ -species atoms. Equations (5) and (6) constitute a closed set of equations for the correlation functions. In contrast to the mean spherical approximation, an analytic solution to the HNC equation is not available, so that it must be solved numerically.

The numerical solution was carried out for the nodal functions $\omega_{\mu\nu}(r) [\equiv h_{\mu\nu}(r) - c_{\mu\nu}(r)]$, with the HNC equation (5) rewritten in the form of

$$c_{\mu\nu}(r) = \exp[-\phi_{\mu\nu}(r)/k_B T + \omega_{\mu\nu}(r)] - \omega_{\mu\nu}(r) - 1. \quad (7)$$

The Ornstein-Zernike relation (6) supplementing Eq. (7) reduces to a simple product form in wave-number space:

$$\bar{\Omega}(q) = [1 - \bar{C}(q)]^{-1} \bar{C}(q) - \bar{C}(q). \quad (8)$$

Here a matrix representation is used, i.e.,

$$\bar{\Omega}(q) = \begin{pmatrix} \Omega_{11}(q) & \Omega_{12}(q) \\ \Omega_{21}(q) & \Omega_{22}(q) \end{pmatrix}, \quad (9)$$

and the Fourier transformation is defined as

$$\Omega_{\mu\nu}(q) = (\rho_\mu \rho_\nu)^{1/2} \int d\mathbf{r} \omega_{\mu\nu}(r) e^{iq \cdot r}. \quad (10)$$

The additional Fourier transformations which are necessary for executing the iteration can be speeded up by adopting the fast-Fourier-transform (FFT) algorithm. The utility of $\omega_{\mu\nu}(r)$ results from the fact that they are continuous functions of r even for hard spheres,²¹ so that their Fourier transforms are shorter range than those for the total and direct correlation functions.

The primitive iteration procedures do not work well because of the strong attractive part involved in the potential between unlike species. To handle such a numerical instability, we used the efficient Newton-Raphson method implemented by Abernethy and Gillan^{22,23} for solving the fluid integral equations. In addition, the long-range problem posed by the Coulombic part in $\phi_{\mu\nu}(r)$ was solved with Ng's method.²⁴ The HNC approximation can be improved by incorporating higher-order corrections and the effect of three-body potentials.²⁵

IV. RESULTS AND DISCUSSION

The HNC equation was solved for a series of R ranging from 0.25 and 3.0, while the other parameters η and Γ

were kept constant. Such a calculation gives definite insight into the size effects on the structural correlations in the system. The fixed parameters coincided with those for the molten GeSe_2 , that is, $\eta=0.44$ and $\Gamma=80$. The numerical integrations in the iteration procedure were carried out at 1024 mesh points with an increment of $\Delta r=0.05a$ ($\Delta q=\pi/1024\Delta r$) in real (wave-number) space. We judged that convergence of the numerical solutions had been achieved when the relative variance between the input and output functions became less than 10^{-5} .

A. Partial pair-distribution functions

The partial pair-distribution functions $g_{\mu\nu}(r)$ are shown in Figs. 1 and 2 for various values of R , where the distance is normalized with sum of the two radii, $d=\sigma_A+\sigma_X$. Because of the very nature of the charged-hard-sphere model, the AX correlation is always well defined. The second shell of X atoms around an A atom is also appreciable for small R . For larger R values, however, the second peak begins to lose a well-defined shell structure. The $X-X$ pair-distribution function has a prominent peak for small R . In addition, on the right-hand side of the peak, we find a shoulder around $r/d=2.0$. For increasing values of R , the height of the peak decreases. The shoulder incidentally becomes more pronounced and in the vicinity of $R=0.75$ it becomes a clearly independent peak. The position of the first peak also shifts toward lower values of r/d as R increases, and for $R>1.0$ the $X-X$ peak is located inside the first shell of the $A-X$ coordination. For small R the first peak in $g_{AA}(r)$ is broad as compared with those in the $A-X$ and

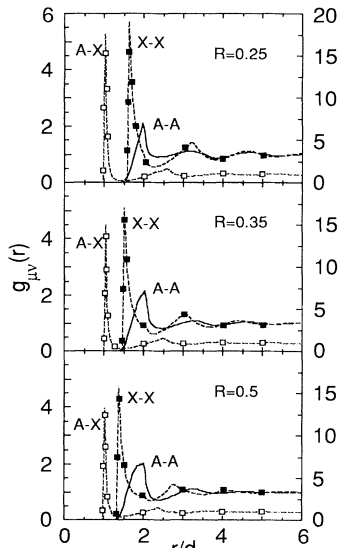


FIG. 1. Partial pair-distribution functions $g_{\mu\nu}(r)$ vs dimensionless distance r/d for AX_2 system from the charged-hard-sphere model for $R=0.25, 0.35,$ and 0.5 , where R denotes the ratio of hard-sphere radii, σ_A/σ_X , and d is the sum of the two radii, $d=\sigma_A+\sigma_X$. Note that the left-hand vertical scale is for $g_{AA}(r)$ and $g_{XX}(r)$, whereas the right-hand scale is for $g_{AX}(r)$.

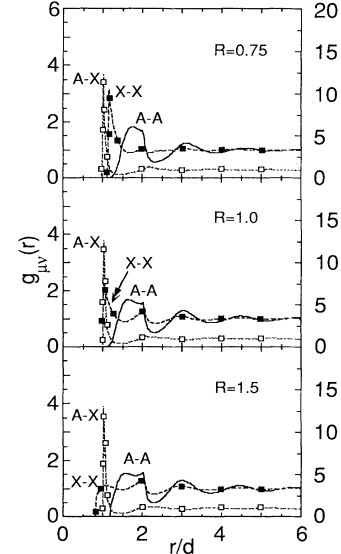


FIG. 2. Partial pair-distribution functions $g_{\mu\nu}(r)$, for $R=0.75, 1.0,$ and 1.5 . Same notation and scales are used as in Fig. 1.

$X-X$ correlations. In addition, the $A-A$ peak becomes broader with increasing R , ultimately being almost square shaped at $R=1.5$.

B. Bond lengths and $A-X$ coordination

The coordination number $N_{\mu\nu}$ of the ν th species around an atom of the μ th species is obtained by integrating the corresponding partial pair-distribution function $g_{\mu\nu}(r)$ as

$$\begin{aligned} N_{\mu\nu} &= 4\pi\rho_\nu \int_0^{r_{\min}} dr r^2 g_{\mu\nu}(r) \\ &= \frac{2c_\nu}{\pi} \int_0^{r_{\min}} dq [S_{\mu\nu}(q) - \delta_{\mu\nu}] \\ &\quad \times \frac{\sin(qr_{\min}) - qr_{\min} \cos(qr_{\min})}{q} + \frac{4\pi}{3} r_{\min}^3 \rho_\nu. \end{aligned} \quad (11)$$

The upper limit r_{\min} of the integration defines the first coordination shell, which was chosen to coincide with the first minimum in $g_{\mu\nu}(r)$. The second expression on the right-hand side of Eq. (11) was employed for the practical calculation to get rid of the discontinuity involved in $g_{\mu\nu}(r)$ due to the hard-core interactions.

We evaluated the bond lengths $d_{\mu\nu}$ between atoms of the μ th and ν th species by averaging the distance around the first peak of $g_{\mu\nu}(r)$ as

$$d_{\mu\nu} = \frac{4\pi\rho_\nu}{N_{\mu\nu}} \int_0^{r_{\min}} dr r^3 g_{\mu\nu}(r). \quad (12)$$

This is because the first peaks in $g_{\mu\nu}(r)$ are significantly distorted (away from a symmetric form) by the existence of hard cores so that the first-peak position provides no appropriate estimate for the bond lengths.

Figure 3 shows the calculated bond lengths and $A-X$

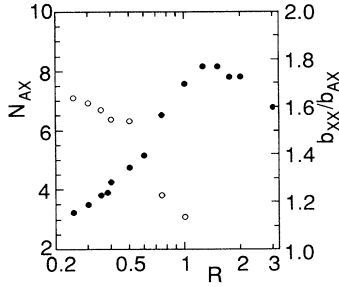


FIG. 3. Coordination number of X atoms around an A atom, N_{AX} (solid circles), and the ratio of calculated X - X to A - X bond lengths, b_{XX}/b_{AX} (open circles), vs R .

coordination number as a function of R . In the absence of a clearly defined peak around $r/d=2.0$ in $g_{XX}(r)$, the X - X bond length was calculated by treating the entire first peak as one entity. For larger values of R when the shoulder at $r/d=2.0$ becomes very pronounced and the value at the dip between the two peaks becomes less than unity, the bond length was calculated using only the main peak (up to the dip).

The A - X coordination is nearly 4 and the ratio of X - X to A - X bond lengths, b_{XX}/b_{AX} , is around 1.6 for $0.25 \leq R \leq 0.4$, so that one can expect that tetrahedral units of $A(X_{1/2})_4$ are built in the system. Even for $R \leq 0.5$ ($\sigma_A \ll \sigma_X$), the A - A distance is larger than the X - X distance. This is also consistent with the formation of well-defined elementary units $A(X_{1/2})_4$. As R increases beyond $R=0.4$, the A - X coordination number exceeds 4 and the ratio of the two bond lengths decreases below 1.6. This indicates a gradual loss of the tetrahedral coordination with the increase of R .

C. Static-structure factors

The partial static-structure factors $S_{\mu\nu}(q)$ are related to $g_{\mu\nu}(r)$ through

$$S_{\mu\nu}(q) = \delta_{\mu\nu} + 4\pi(\rho_\mu\rho_\nu)^{1/2} \int_0^\infty dr r^2 [g_{\mu\nu}(r) - 1] \frac{\sin(qr)}{qr}. \quad (13)$$

Since $g_{\mu\nu}(r)$ have a long-lived oscillatory tail at long distances, expression (13) is not suitable to the numerical computation of $S_{\mu\nu}(q)$. Here we instead calculated $S_{\mu\nu}(q)$ from the direct correlation functions $c_{\mu\nu}(r)$ using the relation

$$\bar{S}(q) = [1 - \bar{C}(q)]^{-1}. \quad (14)$$

The accurate Fourier transforms of $c_{\mu\nu}(r)$ are obtainable as a simultaneous result of the present numerical solution scheme for the HNC equation.

To analyze the nature of structural correlations in the system in terms of the number- and charge-density fluctuations, we introduce the additional static-structure factors

$$S_{NN}(q) = \sum_{\mu\nu} (c_\mu c_\nu)^{1/2} S_{\mu\nu}(q), \quad (15)$$

$$S_{ZZ}(q) = \frac{1}{\langle Z^2 \rangle} \sum_{\mu\nu} Z_\mu Z_\nu (c_\mu c_\nu)^{1/2} S_{\mu\nu}(q), \quad (16)$$

$$S_{NZ}(q) = \frac{1}{\langle Z^2 \rangle^{1/2}} \sum_{\mu\nu} (c_\mu c_\nu)^{1/2} Z_\nu S_{\mu\nu}(q), \quad (17)$$

where $\langle Z^2 \rangle = \sum_\mu c_\mu Z_\mu^2$. Number-density wave fluctuations such as medium-range order in glasses appear in the form of a prominent peak in $S_{NN}(q)$. The strength of charge ordering is measured by $S_{ZZ}(q)$. To what extent cross coupling between the number and charge fluctuations takes place is described by $S_{NZ}(q)$.

All of the structure factors are shown in Figs. 4–7 for six values of R in $0.25 \leq R \leq 1.5$. Distinguished features of those structure factors are observed in the range of $qd < 9$. The A - A partial structure factors in Fig. 4 show two peaks at $R=0.25$, which slowly merge into a single peak as R increases to 0.5. Since the first peaks in $S_{AA}(q)$ and $S_{AX}(q)$ are located at a different position from the first peak in $S_{XX}(q)$ for $R \leq 0.5$, the total structure factor $S_{NN}(q)$ in Fig. 6 has three peaks in the range $qd < 9$; those two first peaks in the A - A and A - X correlations give rise to the FSDP in $S_{NN}(q)$. The partial structure factors in Fig. 5 at $R=0.75, 1.0$, and 1.5 are qualitatively different from those in Fig. 4. For $R=1.0$ and 1.5 , the first peak in $S_{AA}(q)$ is more dominant than the first peak in $S_{XX}(q)$ and the two peaks are at the same position. This results in a single-peak structure in $S_{NN}(q)$ for $qd < 9$ at the corresponding values of R in Fig. 7.

The structure factors $S_{AA}(q)$ and $S_{XX}(q)$ are positive definite for all values of q , whereas $S_{AX}(q)$ can be of either sign. In Fig. 4 (for $R \leq 0.5$), the main peak in the X - X correlation at $qd \approx 4.5$ is accompanied by a deep valley in the A - X correlation. This is a manifestation of charge ordering in the system, which is common to dense

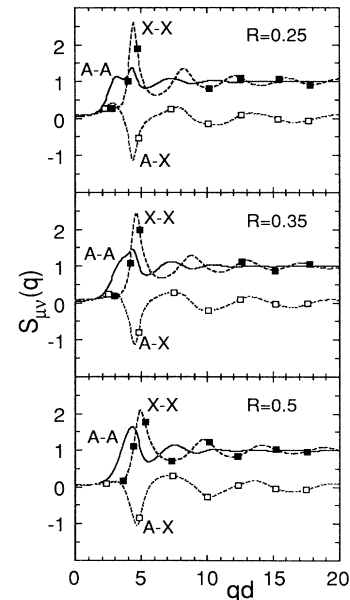


FIG. 4. Partial static-structure factors $S_{\mu\nu}(q)$ for $R = 0.25, 0.35$, and 0.5 .

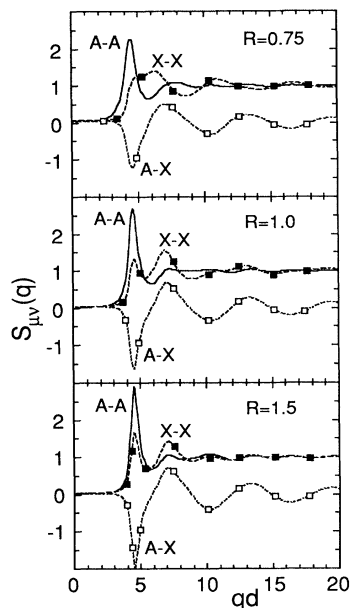


FIG. 5. Partial static-structure factors $S_{\mu\nu}(q)$ for $R = 0.75$, 1.0, and 1.5.

ionic systems.²¹ For larger values of R , in Fig. 5, the same features are displayed, but with the A - A and A - X correlations. This signifies that A -species atoms take over the dominant role in determining the correlation structure of the system from X -species atoms somewhere between $R = 0.5$ and 0.75.

It is clear from $S_{NN}(q)$ in Fig. 6 that the FSDP is present at $R = 0.25$ and its position is $qd = 3.0$. With in-

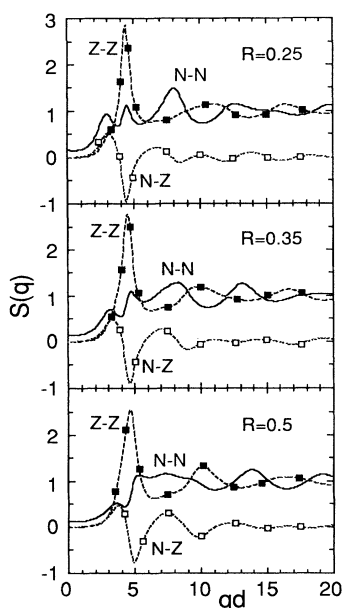


FIG. 6. Charge-number structure factors for $R = 0.25$, 0.35, and 0.5. The solid curve stands for the number-number structure factor $S_{NN}(q)$, the dashed curve for the charge-charge structure factor $S_{ZZ}(q)$, and the dotted curve for the cross-correlation function $S_{NZ}(q)$.

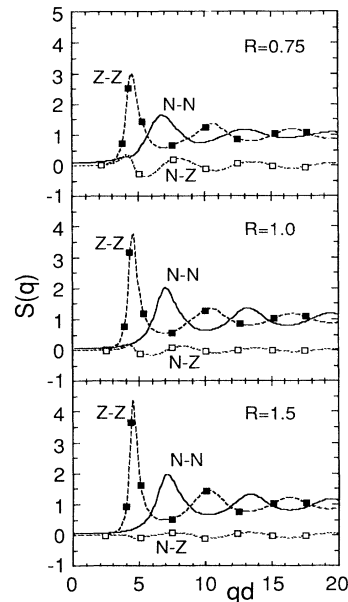


FIG. 7. Charge-number structure factors for $R = 0.75$, 1.0, and 1.5. Same notation is used as in Fig. 6.

creasing R the height of the FSDP goes down and the peak broadens; in addition, the position of the FSDP shifts to larger values of qd (3.0–3.6 as R increases from 0.25 to 0.5). It should also be iterated here that, for $R \leq 0.5$, $S_{NN}(q)$ has three peaks in $qd < 9$. These systems model those glasses such as SiO_2 , SiS_2 , SiSe_2 , GeO_2 , GeS_2 , and GeSe_2 , which show the FSDP's in their scattering functions. On the other hand, for $R = 1.0$ and 1.5, there is only one peak in $S_{NN}(q)$ in the same range of q . As we have indicated earlier, $R \geq 1.0$ leads to disordered Ag_2Se -type structures; the correlation functions at $R = 1.5$ are generally in good agreement with those of molten Ag_2Se , which were obtained by molecular-dynamics (MD) simulations.²⁰ We can thus conclude that the regimes of $R \leq 0.5$ and $R \geq 1.0$ represent two entirely different classes of systems; $R = 0.75$ is in the transition region between SiO_2 - and Ag_2Se -type disordered structures.

The charge-charge structure factor in Figs. 6 and 7 shows basically the same structure for all values of R . The charge-charge correlation function has no peak corresponding to the FSDP; for $qd < 9$, there is a single peak in the entire range of R . This result, when combined with the observation of the FSDP in $S_{NN}(q)$, means that the length scale responsible for the FSDP is charge neutral; i.e., it shows no significant charge-charge fluctuations for the wave number at which the FSDP is seen.

The cross-correlation function $S_{NZ}(q)$ is also displayed in Figs. 6 and 7. For $R \leq 0.5$, considerable coherence in phase between the number and charge fluctuations is observed at the FSDP position; the charge-density fluctuations associated with medium-range order are of no significance in its strength, though. We also note that in the same range of R the principal peak in $S_{ZZ}(q)$, reflecting the charge ordering, is attended by the anticorrelation peak in $S_{NZ}(q)$. Beyond $R = 1.0$, in con-

trast, the structural properties of the system are almost independently described in terms of the two density fluctuations, which are quite similar to those of symmetric molten salts.²¹

D. Medium-range correlations and charge ordering

From the above examination of the partial structure factors and number-number and charge-charge structure factors, it is clear that the FSDP only occurs in $S_{NN}(q)$ for $R \leq 0.5$. The height of the FSDP along with its full width at half maximum (FWHM) is shown in Fig. 8. It is quite remarkable that when going from $R = 0.25$ (where the elementary unit, a tetrahedron, is well defined) to $R = 0.5$ (where the A - X coordination number is around 5), the height of the FSDP drops to almost half of its value and the peak width increases by a factor of 2. For $R > 0.5$ the FSDP is absent, signifying a total loss of intermediate-range order. We thus see the intimate relationship between the existence of basic structural units and the appearance of the FSDP.

In the charged-hard-sphere model, the position of the FSDP is found at $qd = 3.0$ at $R = 0.25$, whereas in the scattering experiments the FSDP is observed around $qd = 2.5$ as shown by Moss and Price.¹ This discrepancy can be easily understood on the basis of three-body covalent forces. In a -GeSe₂, with only two-body interaction potentials being used in the MD simulations,¹⁵ the position of the FSDP was determined to be $q = 1.4 \text{ \AA}^{-1}$, which implies $qd = 1.4 \times 2.35 = 3.0$. Inclusion of three-body covalent forces then moved the position of the FSDP from 1.4 to 1.0 \AA^{-1} in complete agreement with the neutron-diffraction experiments.¹⁶ This result leads to $qd = 1.0 \times 2.35 = 2.35$, which agrees with the elucidation by Moss and Price. Therefore the FSDP position obtained in the charged-hard-sphere model without three-body interactions is quite consistent with the MD and experimental results.

The nature of charge ordering is summarized in Fig. 9, which shows the height of the first peak and its FWHM in the charge-charge structure factor $S_{ZZ}(q)$. We can divide the range of $R = 0.25$ – 3.0 into three regions in accordance with the classification in $S_{NN}(q)$. In the first re-

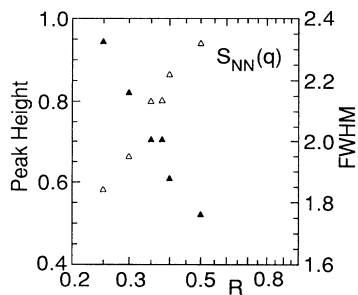


FIG. 8. Peak height and full width at half maximum (FWHM) of the FSDP in the number-number structure factor as a function of R . The solid and open triangles are for the peak height and FWHM, respectively.

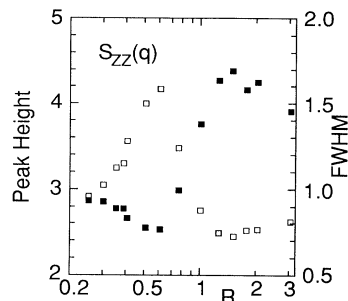


FIG. 9. Peak height and full width at half maximum (FWHM) of the first peak in the charge-charge structure factor as a function of R . The solid and open squares are for the peak height and FWHM, respectively.

gion $0.25 \leq R \leq 0.5$, the height of the first peak decreases and its width increases, indicating a reduction of charge ordering. It is this region of R where one observes the FSDP in $S_{NN}(q)$. The FSDP also shows a similar behavior in this region. The second region $0.5 < R < 1.0$ represents a regime where there is a frustration in charge ordering because of competition between the steric effects and Coulomb interactions. The third region of $R \geq 1.0$ has good charge ordering where the height of the first peak is large and the width is small.

The excess number function²⁶ for A -species atoms defined by

$$\delta N_{AA}(r) = 1 + 4\pi\rho_A \int_0^r dr_1 r_1^2 [g_{AA}(r_1) - 1] \quad (18)$$

is shown for $R = 0.25$ – 1.5 in Fig. 10. For $R > 0.5$ the envelop of the function shows marked exponential decay as a function of r/d . The situation is quite different for $R \leq 0.5$. The envelop function is nonmonotonic, and the

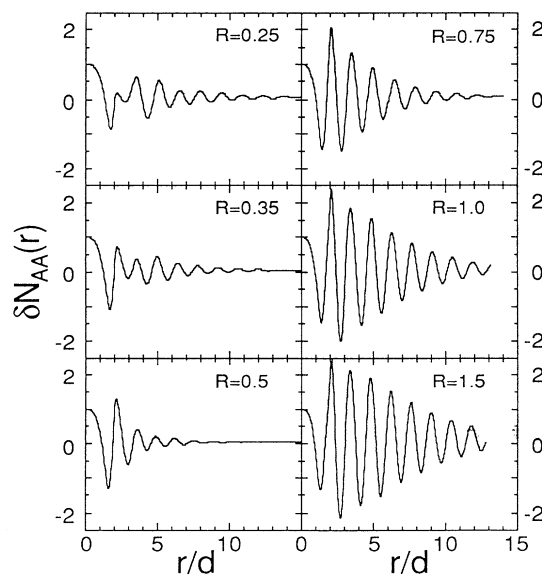


FIG. 10. Excess number function for A -type atoms, $\delta N_{AA}(r)$, vs dimensionless distance r/d .

excess number function shows considerable enhancement in the region of $r/d \approx 5$. It is also this range of R values in which the number-number structure factor shows the FSDP.

V. CONCLUSION

Figures 3, 8, and 9 summarize the dependence of the structure on relative steric sizes in AX_2 -type mixtures of charged hard spheres. Combining these results, we can illustrate the definite structural change as a function of the atomic-radius ratio R which spans the range $0.25 \leq R \leq 3.0$.

In the first region of $0.25 \leq R \leq 0.5$, the A - X coordination is around 4 along with $b_{XX}/b_{AX} \approx 1.6$, indicating a well-defined tetrahedral elementary unit $A(X_{1/2})_4$. The number-number structure factor shows the FSDP in this region. As R increases from 0.25 toward 0.5, however, the height of the FSDP decreases with an increase of the FWHM and the position of the FSDP shifts to larger values of q . The number-number structure factor has three peaks for $qd < 9$ in this range of R . The charge-charge structure factor, on the other hand, has only one peak for $qd < 9$ in the entire R range of 0.25–3.0. For $0.25 < R < 0.5$, the charge ordering decreases, which is indicated by the depression of the first peak in $S_{ZZ}(q)$.

In the second region $0.5 < R < 1.0$, the A - X coordination number changes from 4 to 8 and correspondingly the ratio of X - X to A - X bond lengths decreases from its

tetrahedral value of 1.6 as R increases from 0.5 to 1.0. The FSDP in the number-number structure factor disappears and the three peaks in $S_{NN}(q)$ for $qd < 9$ merge into one peak in this R range; the intermediate-range order is completely destroyed. The charge ordering shows frustration, which is manifested by the relatively large width and small height of the first peak in $S_{ZZ}(q)$. This is due to competition between steric and Coulomb interactions in this second range of R , leading to the structural change from fourfold to eightfold A - X coordination.

In the third region $1.0 \leq R \leq 3.0$, the A - X coordination is around 8 and there is no FSDP in $S_{NN}(q)$; one can see no intermediate-range order in this range either as for the second range of R . The number-number structure factor is relatively structureless; it has only a single peak in the range of $qd < 9$. There is, however, excellent charge ordering in this range of R as shown by the large height and small FWHM of the first peak in $S_{ZZ}(q)$, while the number and charge fluctuations are nearly decoupled.

ACKNOWLEDGMENTS

The authors would like to thank Dr. Aiichiro Nakano for a critical reading of the manuscript and his help in preparation of the figures. This work was partially supported by the U.S. Department of Energy, Office of Energy Research, Basic Energy Science, Materials Science Division, Grant No. DE-FG05-92ER45477.

- ¹S. C. Moss and D. L. Price, in *Physics of Disordered Materials*, edited by D. Adler, H. Fritzsche, and S. R. Ovshinsky (Plenum, New York, 1985), p. 77.
- ²D. L. Price, S. C. Moss, R. Reijers, M.-L. Saboungi, and S. Susman, *J. Phys. C* **21**, L1069 (1988).
- ³H. Iyetomi, P. Vashishta, and R. K. Kalia, *J. Phys. Condens. Matter* **1**, 2103 (1989).
- ⁴H. Iyetomi, P. Vashishta, and R. K. Kalia, *Phys. Rev. B* **43**, 1726 (1991).
- ⁵G. D. Mahan and W. L. Roth, *Superionic Conductors* (Plenum, New York, 1976).
- ⁶P. Vashishta, J. N. Mundy, and G. K. Shenoy, *Fast Ion Transport in Solids* (North-Holland, Amsterdam, 1979).
- ⁷M. B. Salamon, *Physics of Superionic Conductors* (Springer, Berlin, 1979).
- ⁸J. M. J. Van Leeuwen, J. Groeneveld, and J. De Boer, *Physica* **25**, 792 (1959).
- ⁹T. Morita, *Prog. Theor. Phys.* **23**, 829 (1960).
- ¹⁰M. Baus and J.-P. Hansen, *Phys. Rep.* **59**, 1 (1980).
- ¹¹S. Ichimaru, H. Iyetomi, and S. Tanaka, *Phys. Rep.* **149**, 91 (1987).
- ¹²M. C. Abramo, C. Caccamo, and G. Pizzimenti, *J. Phys. C* **13**, 5473 (1980).
- ¹³G. Pastore, P. Ballone, and M. P. Tosi, *J. Phys. C* **19**, 487 (1986).
- ¹⁴P. Ballone, G. Pastore, J. S. Thakur, and M. P. Tosi, *Physica* **142B**, 294 (1986).
- ¹⁵P. Vashishta, R. K. Kalia, and I. Ebbsjö, *Phys. Rev. B* **39**, 6034 (1989).
- ¹⁶P. Vashishta, R. K. Kalia, G. A. Antonio, and I. Ebbsjö, *Phys. Rev. Lett.* **62**, 1651 (1989).
- ¹⁷M. C. Abramo, C. Caccamo, G. Pizzimenti, M. Parrinello, and M. P. Tosi, *J. Phys. C* **9**, L593 (1976).
- ¹⁸M. C. Abramo, C. Caccamo, G. Pizzimenti, M. Parrinello, and M. P. Tosi, *J. Chem. Phys.* **68**, 2889 (1978).
- ¹⁹E. Waisman and J. L. Lebowitz, *J. Chem. Phys.* **56**, 3086 (1972).
- ²⁰J. P. Rino, Y. M. M. Hornos, G. A. Antonio, I. Ebbsjö, R. K. Kalia, and P. Vashishta, *J. Chem. Phys.* **89**, 7542 (1988).
- ²¹J. P. Hansen and I. R. McDonald, *Theory of Simple Liquids* (Academic, London, 1986).
- ²²M. J. Gillan, *Mol. Phys.* **38**, 1781 (1979).
- ²³G. M. Abernethy and M. J. Gillan, *Mol. Phys.* **39**, 839 (1980).
- ²⁴K.-C. Ng, *J. Chem. Phys.* **61**, 2680 (1974).
- ²⁵H. Iyetomi and P. Vashishta, *Phys. Rev. A* **40**, 305 (1989).
- ²⁶M. Dixon and R. M. Atwood, *Phys. Chem. Liq.* **6**, 189 (1977).